

Discovery and Characterization of a Highly Selective FAAH Inhibitor that Reduces Inflammatory Pain

Kay Ahn,^{1,*} Douglas S. Johnson,¹ Mauro Mileni,² David Beidler,³ Jonathan Z. Long,⁴ Michele K. McKinney,⁴ Eranthie Weerapana,⁴ Nalini Sadagopan,⁵ Marya Liimatta,⁶ Sarah E. Smith,³ Scott Lazerwith,⁵ Cory Stiff,¹ Satwik Kamtekar,³ Keshab Bhattacharya,³ Yanhua Zhang,¹ Stephen Swaney,⁵ Keri Van Becelaere,⁵ Raymond C. Stevens,^{2,*} and Benjamin F. Cravatt^{4,*}

¹Pfizer Global Research and Development, Groton, CT 06340, USA

²Department of Molecular Biology, The Scripps Research Institute, 10550 North Torrey Pines Road, La Jolla, CA 92037, USA

³Pfizer Global Research and Development, Chesterfield, MO 63017, USA

⁴The Skaggs Institute for Chemical Biology and Department of Chemical Physiology, The Scripps Research Institute, 10550 North Torrey Pines Road, La Jolla, CA 92037, USA

⁵Pfizer Global Research and Development, Ann Arbor, MI 48105, USA

⁶Pfizer Global Research and Development, Cambridge, MA 02139, USA

*Correspondence: kay.ahn@pfizer.com (K.A.), stevens@scripps.edu (R.C.S.), cravatt@scripps.edu (B.F.C.)

DOI 10.1016/j.chembiol.2009.02.013

SUMMARY

Endocannabinoids are lipid signaling molecules that regulate a wide range of mammalian behaviors, including pain, inflammation, and cognitive/emotional state. The endocannabinoid anandamide is principally degraded by the integral membrane enzyme fatty acid amide hydrolase (FAAH), and there is currently much interest in developing FAAH inhibitors to augment endocannabinoid signaling in vivo. Here, we report the discovery and detailed characterization of a highly efficacious and selective FAAH inhibitor, PF-3845. Mechanistic and structural studies confirm that PF-3845 is a covalent inhibitor that carbamylates FAAH's serine nucleophile. PF-3845 selectively inhibits FAAH in vivo, as determined by activity-based protein profiling; raises brain anandamide levels for up to 24 hr; and produces significant cannabinoid receptor-dependent reductions in inflammatory pain. These data thus designate PF-3845 as a valuable pharmacological tool for in vivo characterization of the endocannabinoid system.

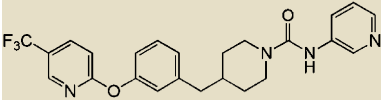
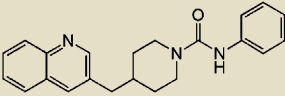
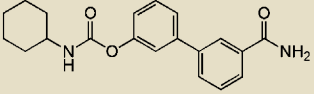
INTRODUCTION

The endogenous cannabinoid (endocannabinoid) system is composed of two G protein-coupled receptors, CB1 and CB2; their cognate lipid ligands *N*-arachidonoyl ethanolamine (anandamide [AEA]) and 2-arachidonoylglycerol (2-AG); and the metabolic enzymes responsible for AEA and 2-AG biosynthesis and degradation (Fowler, 2006; Pacher et al., 2006; Di Marzo et al., 2007; Ahn et al., 2008). CB1 and CB2 are also activated by Δ^9 -tetrahydrocannabinol (THC), the psychoactive substance in marijuana (Mechoulam, 1986). THC and other direct CB1 agonists have long been recognized to possess medicinally beneficial properties, such as pain relief; however, these agents

also produce myriad side effects, including impairments in cognition and motor control, that limit their broad clinical utility. In contrast, inhibitors of the principal AEA-degrading enzyme fatty acid amide hydrolase (FAAH) (Cravatt et al., 1996; McKinney and Cravatt, 2005) and FAAH(−/−) mice have been found to display analgesia (Cravatt et al., 2001; Kathuria et al., 2003; Lichtman et al., 2004a, 2004b; Chang et al., 2006; Russo et al., 2007), anti-inflammation (Cravatt et al., 2004; Massa et al., 2004; Holt et al., 2005), anxiolysis (Kathuria et al., 2003; Naidu et al., 2007; Moreira et al., 2008), and antidepressant (Gobbi et al., 2005; Naidu et al., 2007) without disruptions in motility, cognition, or body temperature (Boger et al., 2000; Cravatt et al., 2001; Kathuria et al., 2003; Lichtman et al., 2004a). These initial findings suggest that FAAH/AEA signaling pathways regulate a discrete subset of the behavioral processes affected by direct CB1 agonists. The selective pharmacological blockade of FAAH has, therefore, emerged as an exciting strategy by which to discern the endogenous functions of AEA-mediated endocannabinoid pathways and gauge their therapeutic potential.

Several classes of FAAH inhibitors have been reported, including reversibly (e.g., α -keto heterocycles [Boger et al., 2000; Leung et al., 2003; Lichtman et al., 2004a]; trifluoromethyl ketones [Koutek et al., 1994; Boger et al., 1999; Leung et al., 2003]) and irreversibly (e.g., carbamates [Kathuria et al., 2003]; fluorophosphonates [Deutsch et al., 1997]) acting agents. These inhibitors each possess distinct sets of attributes and deficiencies that reflect some of the most challenging aspects of FAAH inhibitor development. Reversible inhibitors, such as the α -keto heterocycle OL-135, have been found to display excellent selectivity for FAAH relative to other serine hydrolases in mammalian proteomes, but they produce only transient elevations in AEA in vivo (Lichtman et al., 2004a). The submaximal efficacy of reversible FAAH inhibitors may be due to their rapid metabolism, as well as to the fact that a near-complete (>85%) blockade of FAAH activity is required to maintain elevated AEA levels in vivo (Fegley et al., 2005). Another challenge with developing reversible inhibitors is that inhibition of FAAH leads to elevated levels of several *N*-acyl ethanolamine (NAE) substrates,

Table 1. Potency, Defined by k_{inact}/K_i Values, Comparison of FAAH Inhibitors PF-3845, PF-750, and URB597

Inhibitor	k_{inact} (s^{-1})	K_i (μM)	k_{inact}/K_i ($\text{M}^{-1}\text{s}^{-1}$)
 PF-3845, 10	0.0033 ± 0.0002	0.23 ± 0.03	14,310
 PF-750	-	-	791 ^a
 URB597	0.0033 ± 0.0003	2.0 ± 0.3	1,590

The k_{inact} and K_i values were obtained as described in Supplemental Experimental Procedures. Values are averages \pm SD of three independent experiments.

^a Mileni et al. (2008).

which can diminish the efficiency and potency of the inhibitor by mass-action competition with the substrate (Swinney, 2004). Irreversible inhibitors, such as the carbamate URB597 (Kathuria et al., 2003), produce a more complete blockade of FAAH in vivo, but they also inhibit other serine hydrolases in peripheral tissues, including several carboxylesterases (Lichtman et al., 2004a; Alexander and Cravatt, 2005; Zhang et al., 2007). Considering that FAAH is a serine hydrolase (Patricelli et al., 1999) and that there are > 200 members of this enzyme class in the human proteome, inhibitor selectivity represents a major challenge.

Toward the goal of developing FAAH inhibitors that display optimal efficacy and selectivity, we recently reported a class of piperidine/piperazine ureas that inhibit FAAH with high specificity (Ahn et al., 2007). Here, we report a detailed mechanistic, structural, and pharmacological characterization of the FAAH piperidine urea inhibitor PF-3845. Our data indicate that PF-3845 displays an unprecedented combination of in vivo activity and selectivity, designating this agent as a valuable pharmacological tool for studying FAAH-regulated endocannabinoid pathways.

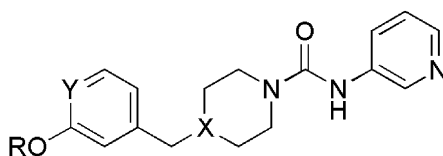
RESULTS AND DISCUSSION

Optimization of Potency of Piperidine/Piperazine Urea FAAH Inhibitors

Recently, we (Ahn et al., 2007) and others (Keith et al., 2008) have described a class of FAAH inhibitors that contain a piperidine/piperazine urea moiety. These agents were found to inhibit FAAH by a covalent, irreversible mechanism involving the carbamylation of FAAH's catalytic S241 nucleophile. Lead urea inhibitors, such as PF-750 (Table 1), however, showed only moderate potency for FAAH, as determined by measurements of k_{inact}/K_i values ($\sim 800 \text{ M}^{-1}\text{s}^{-1}$). In an effort to improve the potency of piperidine/piperazine urea inhibitors, we explored a series of

analogues in which the quinoline group of PF-750 was replaced by a biaryl ether group (Table 2). This medicinal chemistry effort culminated in the discovery of PF-3845 (compound **10**, Table 2), a biaryl ether piperidine that displayed a 10- to 20-fold higher k_{inact}/K_i value for FAAH compared to PF-750 or the well-studied carbamate FAAH inhibitor URB597 (Kathuria et al., 2003) (Tables 1 and 2). Key features of PF-3845 that contribute to enhanced potency include the *p*-trifluoromethyl substituent on the biaryl ether moiety and substitution of the aniline leaving group of PF-750 with 3-aminopyridine.

We next examined the mechanism of FAAH inhibition by PF-3845 in more detail by using an enzyme-coupled assay with oleamide as a substrate, where stoichiometric quantities of NAD^+ are formed upon the generation of ammonia from oleamide by FAAH hydrolysis (Ahn et al., 2007). Linear production of NAD^+ was observed over a 40 min time period in the absence of PF-3845 (see Figure S1A available online). In the presence of PF-3845, the progress curves for oleamide hydrolysis by FAAH exhibited curvature (Figure S1A), consistent with an irreversible mechanism of inhibition. The data were fit to a pseudo-first-order decay equation to determine k_{obs} values at each inhibitor concentration. Plotting these k_{obs} values as a function of PF-3845 concentration revealed saturation (Figure S1B), thus supporting a two-step mechanism for FAAH inactivation involving reversible binding of PF-3845 to FAAH, followed by the second chemical step that results in covalent bond formation. Based on this model, k_{inact} and K_i values for FAAH inhibition by PF-3845 were calculated to be $0.0033 \pm 0.0002 \text{ s}^{-1}$ and $0.23 \pm 0.03 \mu\text{M}$, respectively (Table 1). Similar progress and saturation curves were plotted for inhibition of FAAH by the carbamate inhibitor URB597 (Figures S1C and S1D), generating k_{inact} and K_i values of $0.0033 \pm 0.0003 \text{ s}^{-1}$ and $2.0 \pm 0.3 \mu\text{M}$, respectively (Table 1). These data thus indicate that most, if not all, of the increased potency observed for PF-3845 over URB597 is due to an improvement in binding affinity (K_i value).

Table 2. Structure-Activity Relationship of Biaryl Ether Urea FAAH Inhibitors

Compound	R	Y	X	k_{inact}/K_i ($M^{-1}s^{-1}$)		
				hFAAH	rFAAH	h/rFAAH
1	4-MePh	C	N	1440 ± 260	303 ± 41	974 ± 490
2	4-OMePh	C	N	1370 ± 300	1190 ± 600	1600 ± 340
3	4-CF ₃ Ph	C	N	4070 ± 22	1340 ± 370	-
4	4-CF ₃ -2-pyr	C	N	4160 ± 570	1520 ± 220	-
5	Ph	C	C	1280 ± 390	314 ± 55	-
6	4-MePh	C	C	4640 ± 170	531 ± 37	-
7	4-CF ₃ Ph	C	C	9230 3600	2140 ± 660	-
8	4-FPh	C	C	3460 ± 390	445 ± 110	2470 ± 130
9	2-pyr	C	C	1090 ± 340	76 ± 1	-
10 (PF-3845)	4-CF ₃ -2-pyr	C	C	12,600 ± 3,000	3900 ± 780	13,300 ± 1,300
11	3-CF ₃ -2-pyr	C	C	267 ± 51	86 ± 7	-
12	6-CF ₃ -2-pyr	C	C	438 ± 260	69 ± 25	-
13	4-OMe-2-pyr	C	C	4780 ± 390	2850 ± 170	-
14	4-NH ₂ -2-pyr	C	C	368 ± 140	64 ± 3	-
15	4-MePh	N	N	17 ± 1	11 ± 3	-

Values are averages ± SD of two independent experiments.

Crystal Structure of a PF-3845-FAAH Complex

To gain more detailed insights into the basis for the improved potency of PF-3845, we next determined the crystal structure of a PF-3845-FAAH complex. Here, we used a recently described “humanized” rat-FAAH (h/rFAAH) protein, in which the active site of rat FAAH (rFAAH) has been mutagenically converted to match the active site of human FAAH (hFAAH) (Mileni et al., 2008). Previous studies have confirmed that h/rFAAH maintains the high recombinant expression levels of rFAAH and the inhibitor sensitivity profile of hFAAH (Mileni et al., 2008), thus providing a versatile model for structure-activity relationship (SAR) studies relevant to the human enzyme.

A crystal structure of the PF-3845-h/rFAAH complex was determined at 2.8 Å resolution (see Table S1 for data collection and refinement statistics), revealing a dimeric enzyme with an overall fold that matched those reported in previous FAAH structures (Bracey et al., 2002; Mileni et al., 2008). PF-3845 was found to be covalently attached to the catalytic S241 nucleophile (Patricelli et al., 1999) of h/rFAAH through a carbamate linkage (Figure 1), similar to the previously reported structure of h/rFAAH complexed with PF-750 (Mileni et al., 2008). The 3-aminopyridine leaving group was not observed in the h/rFAAH structure, but the remaining piperidine portion of the parent molecule occupied the acyl chain-binding pocket (Figure 1A). As was observed in the PF-750-h/rFAAH structure (Mileni et al., 2008), a strong aromatic C-H... π interaction (Brandl et al., 2001) can be seen between F192 and the phenyl aromatic ring of PF-3845 (Figure 1A). The ~20-fold improvement in potency for PF-3845 appears to derive from a more extended set of van der Waals

interactions between this inhibitor’s 4-trifluoromethyl-2-pyridyl group and the hydrophobic acyl chain-binding pocket of FAAH (Figure 1B). In this respect, the biaryl ether piperidine moiety of PF-3845 binds in a fashion that more closely resembles the arachidonyl chain of the original methyl arachidonyl phosphonate (MAP)-rFAAH crystal structure (Bracey et al., 2002) (Figure 1C).

One marked difference that we previously observed between the crystal structures of FAAH bound to MAP (Bracey et al., 2002) and PF-750 (Mileni et al., 2008) was that the shorter PF-750 group allowed F432 to undergo a conformational shift that moved this residue out of the membrane access channel and into the acyl chain-binding pocket (Figure 1B). In the PF-3845-h/rFAAH structure, F432 resides in the membrane access channel at a site similar to its position in the MAP-rFAAH structure (Figure 1C). Adjacent to F432, residue M436 also undergoes a rotation of about 135° along the C α -C β axis in both the PF-3845 and MAP-FAAH structures (Figure 1C). The structural rearrangements of F432 and M436 thus appear to occur in a coordinated manner in these three structures and establish that inhibitors can promote conformational shifts that alter the relative size of FAAH’s acyl chain-binding pocket and membrane access channel. The dynamic nature of this region of FAAH could facilitate entrance of lipid substrates from the cell membrane into the enzyme’s active site.

The PF-3845-FAAH structure also aided our understanding of the SAR within the biaryl ether urea series by means of Monte Carlo simulations and energy calculations. For example, these calculations suggest that the higher potency of piperidine ureas

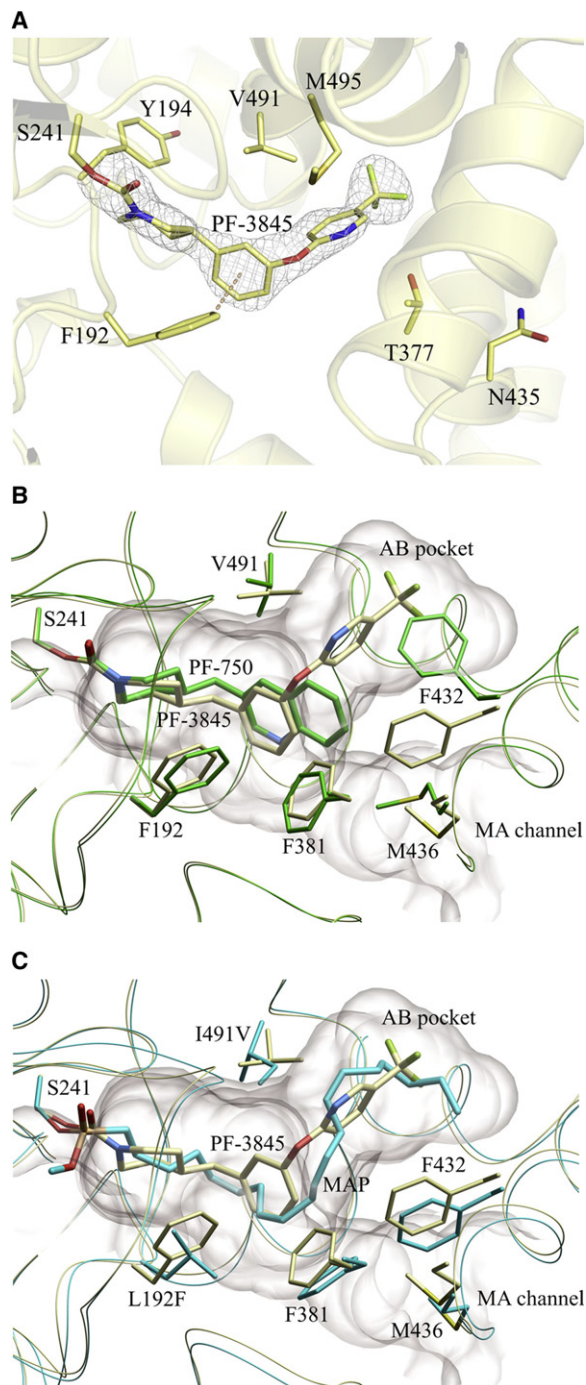


Figure 1. Crystal Structure of a PF-3845-h/rFAAH Complex

(A) Active site image of the PF-3845-h/rFAAH complex, showing the S241-carbamylated adduct and six residues that have been mutated in h/rFAAH.

(B) Overlap of the crystal structures of the PF-3845 (gray) and PF-750 (green) complexes with h/rFAAH, showing the different modes of binding that lead to distinct conformations for the F432 residue that toggles between the membrane access (MA) channel (F432 in gray) and the acyl chain-binding (AB) pocket (F432 in green).

(C) Overlap of the crystal structures of PF-3845-h/rFAAH and MAP-rFAAH complexes, showing similar binding modes for PF-3845 (gray) and MAP (blue).

(compounds **6**, **7**, **10**; Table 2) over the corresponding piperazine ureas (compounds **1**, **3**, **4**; Table 2) is likely due to unfavorable electrostatic interactions of the protonated piperazine within the hydrophobic acyl chain-binding pocket. Furthermore, replacement of the central phenyl group of PF-3845 with a pyridyl group drastically reduces inhibitor potency (compound **15**; Table 2), which may reflect disruption of the aromatic-CH... π interaction with F192 caused by the higher electron withdrawing character of the pyridyl nitrogen, which lessens the electron density of the π ring. Finally, the crystal structure provides an attractive model to explain the improved potency gained by insertion of a trifluoromethyl group at the 4 position of the 2-pyridyl ring that resides in the acyl chain-binding pocket. Reducing the size of this substituent to a methyl or fluoro group decreased inhibitor potency (compounds **6** and **8**, respectively; Table 2), which can be rationalized by simulations that predict suboptimal van der Waals contacts for these smaller groups. Conversely, moving the trifluoromethyl group to the 3 or 6 position, which also impairs potency (compounds **11** and **12**, respectively; Table 2), is predicted to introduce steric clashes with the FAAH protein.

PF-3845 Selectively Inhibits FAAH In Vivo for up to 24 hr

We next administered PF-3845 to mice (10 mg/kg, i.p.) and monitored FAAH inactivation and substrate levels in the brain over a time course from 1 to 24 hr. For comparison, we also analyzed mice treated with URB597 (10 mg/kg, i.p.). Both PF-3845- and URB597-treated mice showed rapid and complete inactivation of FAAH in the brain, as judged by competitive activity-based protein profiling (ABPP) (Liu et al., 1999; Leung et al., 2003) with the serine hydrolase-directed probe fluorophosphonate (FP)-rhodamine (Patricelli et al., 2001) (Figure 2A). PF-3845 showed a longer duration of action than URB597, as judged by the rate of recovery of FP labeling of FAAH. Whereas URB597-treated animals showed nearly wild-type levels of brain FAAH activity by 24 hr, FAAH was still mostly inhibited (>75%) at this time point in PF-3845-treated animals (Figure 2A). These ABPP studies confirmed that PF-3845 and URB597 were both highly selective for FAAH in the brain, since none of the other FP-reactive serine hydrolases in this tissue were inhibited by these agents. In contrast, URB597, but not PF-3845, blocked FP labeling of several additional liver serine hydrolases (Figure 2B), which have previously been identified as carboxylesterases (Alexander and Cravatt, 2005; Zhang et al., 2007). We furthermore tested PF-3845 for the effects on FAAH-2, a recently identified FAAH homolog that is selectively expressed in higher mammals (Wei et al., 2006), but not rodents. In contrast to URB597, which has been found to inhibit human FAAH-2 with high potency (Wei et al., 2006), PF-3845 showed negligible activity against this FAAH variant ($IC_{50} > 10 \mu M$; Figure S2).

To confirm the in vivo selectivity of PF-3845, we synthesized an alkyne analog of this inhibitor, termed PF3845yne (Figure 3A), which maintained high potency for FAAH (k_{inact}/K_i value of $5230 M^{-1}s^{-1}$). We then directly analyzed the protein targets of PF3845yne in vivo by click chemistry (CC)-ABPP (Speers et al., 2003; Speers and Cravatt, 2004; Alexander and Cravatt, 2005). For these studies, we compared the labeling profile of PF3845yne to those of JP104 (Figure 3B), a previously

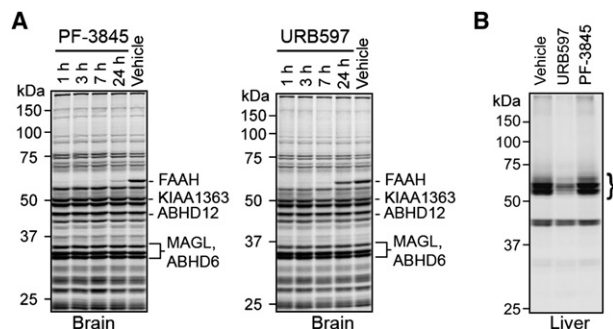


Figure 2. In Vivo Selectivity Analysis for PF-3845 and URB597 as Determined by Competitive ABPP

(A) Gel profiles of FP-rhodamine-labeled brain serine hydrolase activities from mice treated with PF-3845 or URB597 (10 mg/kg, i.p.) for the indicated times. Note that selective blockade of FP-rhodamine labeling of FAAH is observed by both inhibitors. Representative additional brain serine hydrolases are designated based on previous ABPP studies (Blankman et al., 2007; Nomura et al., 2008).

(B) Gel profiles of FP-rhodamine-labeled liver serine hydrolase activities from mice treated with PF-3845 or URB597 (10 mg/kg, i.p., 2 hr). Note that URB597, but not PF-3845, blocks FP-rhodamine labeling of several liver serine hydrolase activities (bracket), which have previously been identified as carboxylesterases (Alexander and Cravatt, 2005; Zhang et al., 2007). For both (A) and (B), fluorescent gel images are shown in grayscale. For (B), a lower scanning intensity is shown due to the highly abundant activity signals for carboxylesterases present in the liver proteome.

described alkyne analog of URB597 (Alexander and Cravatt, 2005). PF3845yne and JP104 were administered to FAAH(+/+) and (–/–) mice (10 mg/kg, i.p.), and, after 2 hr, animals were sacrificed and their brain and liver proteomes analyzed by CC-ABPP by using an azide-rhodamine tag. Consistent with the results of our competitive ABPP experiments (Figure 2), PF3845yne and JP104 selectively reacted with a single protein in mouse brain that was confirmed as FAAH based on its absence in FAAH(–/–) mice (Figure 3C). In liver, however, PF3845yne and JP104 showed strikingly different profiles, with

the former agent once again showing selective reactivity with FAAH and the latter inhibitor labeling a number of proteins that were found in both FAAH(+/+) and (–/–) mice (Figure 3D). A single faint ~60 kDa labeling event was observed in liver proteomes from PF3845yne-treated FAAH(–/–) mice, but a similar signal was also detected in vehicle-treated animals, suggesting that this protein may represent a nonspecific target of the azide-rhodamine tag. Collectively, these data indicate that PF-3845 inhibits FAAH in vivo with exceptional efficacy and selectivity.

FAAH Inhibition by PF-3845 Causes a Dramatic and Sustained Elevation in AEA

Previous studies with FAAH(–/–) mice (Cravatt et al., 2001; Saghatelian et al., 2004) and rodents treated with FAAH inhibitors (Kathuria et al., 2003; Saghatelian et al., 2004) have confirmed a key role for FAAH in regulating tissue levels of AEA and other NAEs. We found that PF-3845-treated mice (10 mg/kg, i.p.) also showed dramatic (>10-fold) elevations in brain levels of AEA (Figure 4A) and other NAEs (*N*-pamitoyl ethanolamine [PEA] [Figure 4B] and *N*-oleoyl ethanolamine [OEA] [Figure 4C]). These animals also showed significant elevations in AEA, PEA, and OEA levels in liver tissue (Figures S3A). In contrast, PF-3845-treated animals did not show changes in the levels of 2-AG in brain or liver (Figure S3B), consistent with previous findings indicating that distinct enzymes regulate this endocannabinoid in vivo (Kathuria et al., 2003; Blankman et al., 2007; Long et al., 2009). We also confirmed that PF-3845 did not alter endocannabinoid (AEA or 2-AG) levels in FAAH(–/–) mice (Figure S3C).

PF-3845-induced elevations in NAEs peaked at ~3 hr and were maintained at maximal levels for up to 7–12 hr, after which they slowly declined. This decline was faster for AEA than for PEA or OEA, possibly reflecting that AEA is a much preferred substrate for FAAH (Cravatt et al., 1996; Wei et al., 2006) and therefore more sensitive to low levels of enzyme recovery. The slightly faster rate of recovery for OEA versus PEA is also

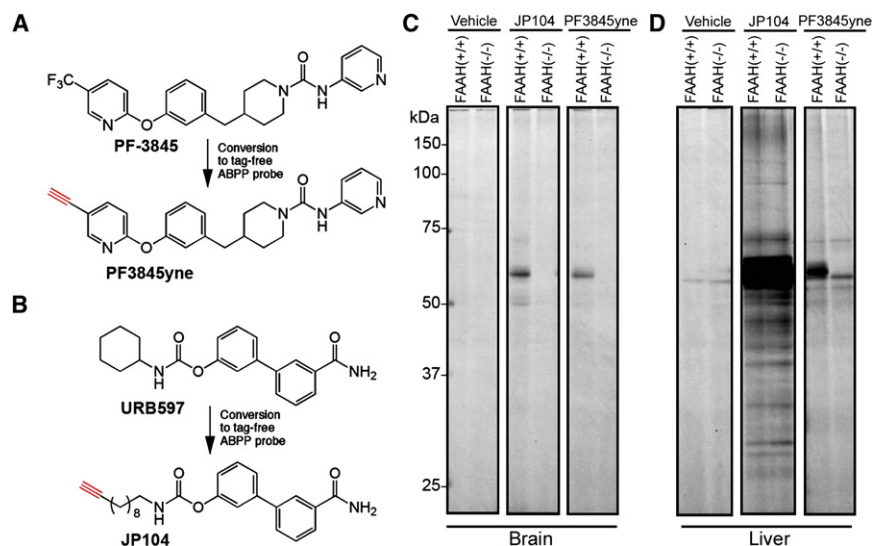


Figure 3. Direct Analysis of In Vivo Protein Targets of Alkyne Analogs of PF-3845 and URB597 by CC-ABPP

(A) Structure of PF3845yne, an alkyne analog of PF-3845.

(B) Structure of JP104, an alkyne analog of URB597 (Alexander and Cravatt, 2005).

(C and D) Gel profiles of CC-ABPP experiments in which (C) brain or (D) liver proteomes from PF3845yne- and JP104-treated mice (10 mg/kg, i.p., 2 hr) were treated with a rhodamine-azide tag under CC conditions and analyzed by in-gel fluorescence scanning (shown in grayscale). PF3845yne selectively labels FAAH in both brain and liver tissue (60 kDa band absent in FAAH(–/–) mice), whereas JP104 labels several additional proteins (protein bands present in both FAAH(+/+) and (–/–) mice). Note that the 55 kDa protein band observed in liver proteome from PF-3845-treated FAAH(–/–) mice was also detected in liver proteomes from vehicle-treated FAAH(+/+) and (–/–) mice and therefore likely represents a background protein that is cross-reactive with the azide-rhodamine tag.

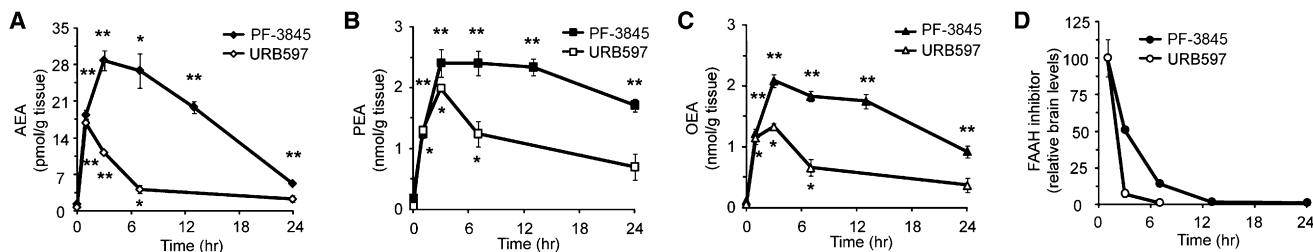


Figure 4. Brain Levels of FAAH Substrates and Inhibitors

(A–C) Brain levels of (A) AEA, (B) PEA, and (C) OEA measured at the indicated time points after treatment with PF-3845 or URB597 (10 mg/kg, i.p.). * $p < 0.05$; ** $p < 0.01$ for inhibitor-versus-vehicle-treated groups. $n = 4$ mice/group.

(D) Brain levels of PF-3845 and URB597 measured at the indicated time points after inhibitor treatment.

consistent with the relative activity that FAAH displays for these substrates in vitro (Wei et al., 2006). Despite FAAH's preference for hydrolyzing AEA, significant elevations in this NAE (as well as PEA and OEA) were still observed at 24 hr posttreatment with PF-3845, consistent with the substantial level of FAAH inhibition maintained at this time point (Figure 2A). URB597-treated mice also showed elevations in NAEs, but these increases were more transient, with AEA levels returning to near-baseline levels by 7 hr posttreatment (Figures 4A–4C). The different rates of recovery of both FAAH activity (Figure 2A) and NAE levels (Figures 4A–4C) in mice treated with PF-3845 versus URB597 likely reflect the distinct half-lives of these inhibitors in vivo, since higher relative brain levels of PF-3845 were maintained over the time course analysis (Figure 4D).

PF-3845 Produces Cannabinoid Receptor-Dependent Reductions in Inflammatory Pain

We next assessed whether PF-3845 was efficacious in a rat model of inflammatory pain. Subcutaneous injection of complete Freund's adjuvant (CFA) into the plantar surface of the hind paw produced a significant decrease in mechanical paw weight threshold (PWT) at 5 days postinjection (Figure 5A). PF-3845 (1–30 mg/kg, oral administration [p.o.]) caused a dose-dependent inhibition of mechanical allodynia with a minimum effective dose (MED) of 3 mg/kg (rats were analyzed at 4 hr post-dosing with PF-3845). At higher doses (10 and 30 mg/kg), PF-3845 inhibited pain responses to an equivalent, if not greater, degree than the nonsteroidal anti-inflammatory drug naproxen (10 mg/kg, p.o.) (Figure 5A). We next determined the relationship between the in vivo efficacy and modulation of FAAH activity and substrates (i.e., NAEs) by PF-3845 in central (brain) and peripheral systems (peripheral blood leukocytes/plasma, liver). Robust, near-complete inhibition of FAAH activity (Figure 5B; Figure S4A) with concomitant elevations in AEA (Figure 5C) and other NAEs (Figures S4B, S4C, and S5) were observed in brain, peripheral blood leukocytes/plasma, and liver from PF-3845-treated animals. Interestingly, we observed a slightly left-shifted dose-response profile for measurements of FAAH activity and NAEs compared to efficacy in the CFA model. For instance, at 1 mg/kg, PF-3845 was found to produce a near-complete blockade of FAAH activity (Figure 5B) and close to maximal elevations in AEA (Figure 5C), but efficacy was not observed at this dose of inhibitor (Figure 5A). These data may indicate the need to fully block FAAH (and fully elevate AEA levels) in order to observe

antiallodynic effects in the CFA model. Alternatively, the kinetics of FAAH blockade may have been slower at lower doses of PF-3845, which could reduce efficacy in pain models that require sustained elevations in AEA. It is also noteworthy that the maximal elevations observed for AEA in PF-3845-treated animals were similar in brain and plasma (~10-fold), whereas OEA and PEA were increased to a lower extent in plasma (~3-fold) compared to brain (~10-fold). This might suggest the existence of alternative degradative (Tsuboi et al., 2005) (or biosynthetic [Leung et al., 2006]) pathways for AEA versus OEA/PEA in peripheral tissues.

Considering that mice treated with PF-3845 showed high (>10-fold) elevations in AEA that lasted for at least 7 hr, we next evaluated the duration of action of this inhibitor in the CFA model from 2–8 hr postadministration. PF-3845 (10 mg/kg, p.o.) exhibited significant inhibition of mechanical allodynia at all time points tested (Figure 5D), although this effect appeared to diminish in magnitude by 8 hr. This loss in activity could reflect gradual recovery of FAAH activity in PF-3845-treated rats, as may be reflected in the decline in AEA levels that was observed at a similar time point in mice treated with this inhibitor (see Figure 4A). However, further time course studies in rats will be required to accurately estimate the duration of action of PF-3845 in these animals. We next examined the involvement of cannabinoid receptors in the PF-3845-induced antiallodynia. Specific antagonists for central CB1 (SR141716) and peripheral CB2 (SR144528) receptors each partially, but significantly, reduced the antiallodynia activity of PF-3845 (Figure 5E). Notably, dual treatment with SR141716 and SR144528 produced a near-complete ablation of the efficacy of PF-3845 in the CFA model (Figure 5E). These data indicate that PF-3845 blocks inflammatory pain responses in the CFA model by a cannabinoid receptor-dependent mechanism that likely involves both CB1 and CB2 receptors, as has been shown for other FAAH inhibitors (Jayamanne et al., 2006).

Conclusions

Endocannabinoids, like other lipid signaling molecules, are thought to be produced on demand by neurons, rather than being stored in synaptic vesicles like classical neurotransmitters (Ahn et al., 2008; Di Marzo, 2008). Although protein-mediated uptake pathways may exist for endocannabinoids (Hillard and Jarrahian, 2003; McFarland and Barker, 2004; Glaser et al., 2005; Fowler, 2006), the hydrophobic nature of these lipids

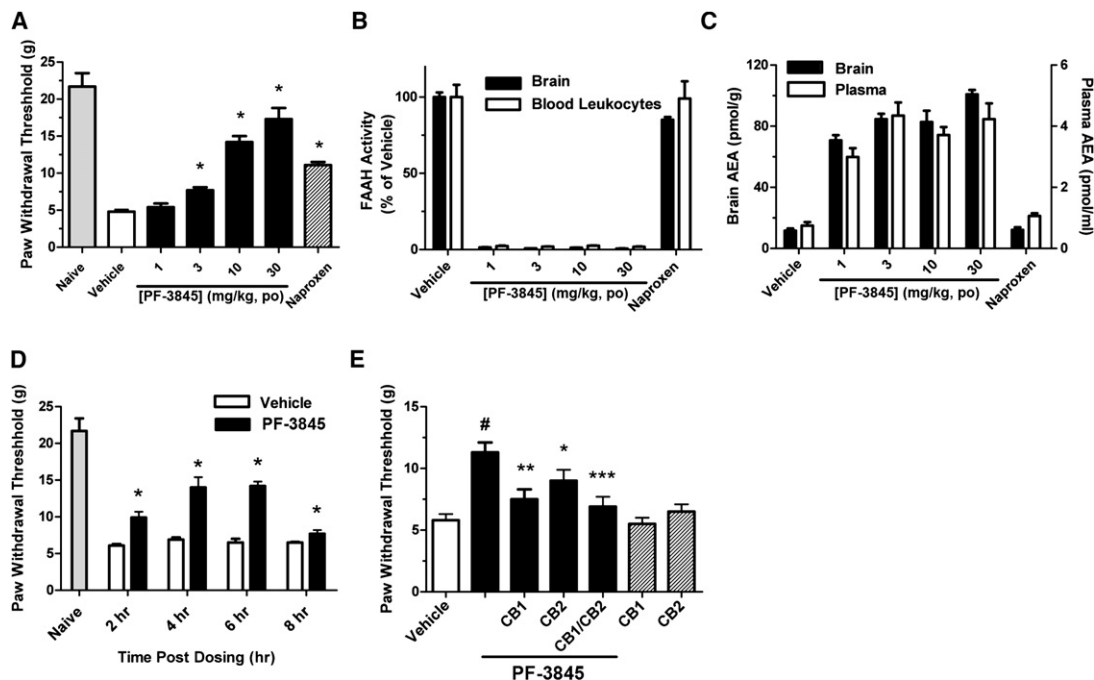


Figure 5. Antihyperalgesic Effects of PF-3845 in the CFA Model of Inflammatory Pain

(A) PF-3845 produces a dose-dependent reduction of mechanical allodynia (hyperalgesia) in rats (black bars). The effect of the nonsteroidal anti-inflammatory drug naproxen (10 mg/kg, p.o., hatched bar) is shown for comparison. Paw-withdrawal thresholds were measured 4 hr postadministration of drugs.

(B and C) PF-3845-treated rats show significant blockade of (B) FAAH activity and elevated (C) AEA levels in brain tissue and blood leukocytes/plasma. All FAAH activity and NAE measurements were determined at 4 hr after drug treatment and were significantly different between PF-3845- and vehicle-treated groups ($p < 0.001$, $n = 3$ rats/group).

(D) Time course for antihyperalgesic effects of PF-3845 (10 mg/kg, p.o.).

(E) Blockade of antihyperalgesic effects of PF-3845 (10 mg/kg, i.p.) by CB1 and CB2 antagonists (SR141716 and SR144528, respectively; 10 and 30 mg/kg, i.p., respectively, administered 1 hr prior to measurement of paw-withdrawal thresholds). Note that neither the CB1 nor the CB2 antagonist displayed significant effects on mechanical allodynia in rats not treated with PF-3845 (hatched bars). # $p < 0.001$, for PF-3845- versus vehicle-treated groups. * $p < 0.05$; ** $p < 0.01$; *** $p < 0.001$, for vehicle-PF-3845- versus CB1/CB2 antagonist-PF-3845-treated groups. $n = 8$ rats/group.

also grants them the ability to freely diffuse across cell membranes. This feature assigns primary responsibility for signal termination to degradative enzymes, such as FAAH. The pharmacological blockade of FAAH has, thus, emerged as a strategy by which to elevate endocannabinoid signaling in vivo and to study the behavioral consequences. Over the past decade, several classes of FAAH inhibitors have been described that vary in their mechanism of action, potency, selectivity, and in vivo efficacy. Arguably, the most well-studied FAAH inhibitor to date is URB597 (Kathuria et al., 2003), a carbamate that irreversibly inhibits FAAH with high selectivity in the nervous system (Alexander and Cravatt, 2005). However, URB597 displays some notable shortcomings, including the inactivation of other serine hydrolases in peripheral tissues (Alexander and Cravatt, 2005; Zhang et al., 2007) and a relatively limited duration of action in vivo. Development of a FAAH inhibitor that displays an optimal combination of efficacy and selectivity has, therefore, remained an intensely pursued objective.

We have described herein the detailed characterization of an advanced piperidine urea inhibitor of FAAH, PF-3845. Our data argue that PF-3845 displays remarkable selectivity for FAAH and robust efficacy in vivo, as reflected in sustained elevations of brain AEA that correlate with cannabinoid receptor-dependent reductions in inflammatory pain responses.

PF-3845 also induces elevations in other noncannabinoid NAEs (e.g., OEA, PEA), which may have additional effects on inflammation and other physiological processes (Lambert et al., 2002). Structural and kinetic studies indicate that the improved potency of PF-3845 compared to previously described inhibitors (URB597, PF-750) likely originates from more extended van der Waals contacts with the hydrophobic FAAH acyl chain-binding tunnel. This premise is also supported by SAR data generated with a set of biaryl ether analogs of PF-3845, in which the introduction of polar groups within certain regions of the inhibitor scaffold severely impaired activity (e.g., compound **16**, Table 2).

In summary, the properties of PF-3845 defined in this study indicate that this agent should be considered a frontline inhibitor for the pharmacological investigation of FAAH-regulated endocannabinoid pathways. Differentiating properties of PF-3845 include its high target selectivity, extended duration of action, and excellent oral bioavailability (>80%, data not shown). These features should make PF-3845 particularly well suited for studying the role of the endocannabinoid system in both central and peripheral physiological processes, as well as chronic pathological syndromes (e.g., neuropathic pain, depression) that may require sustained elevations in endocannabinoid tone for rectification.

SIGNIFICANCE

The endocannabinoid system regulates a number of important physiological processes in mammals and is the principal site of action for THC, the psychoactive ingredient in marijuana. THC and other direct agonists of the CB1 receptor have potentially useful medicinal properties, such as pain relief, but these activities are accompanied by a variety of untoward side effects, including impairment in motor control and cognitive function. In contrast, blockade of endocannabinoid-metabolizing enzymes such as FAAH has been shown to reduce pain sensation, inflammation, and anxiety/depression without substantial effects on motility or cognition. Despite considerable advances in the development of FAAH inhibitors, agents that combine high target selectivity with exceptional *in vivo* efficacy are still needed. Here, we report the discovery and detailed characterization of PF-3845, a piperidine urea FAAH inhibitor that satisfies these criteria. PF-3845 was shown by mechanistic and structural studies to covalently inactivate FAAH by carbamylation of the enzyme's serine nucleophile. PF-3845 completely inhibited FAAH activity, but did not react with other serine hydrolases *in vivo*, as determined by activity-based proteomics; raised brain levels of the endocannabinoid AEA for up to 24 hr; and produced significant CB1/CB2-dependent antihyperalgesic effects in the CFA model of inflammatory pain. From these data, we conclude that PF-3845 is a highly selective and efficacious inhibitor of FAAH that should prove to be a valuable pharmacological tool for investigating the function of the endocannabinoid system.

EXPERIMENTAL PROCEDURES

Materials

N-phenyl-4-(quinolin-3-ylmethyl)piperidine-1-carboxamide (PF-750) was synthesized as described previously (Ahn et al., 2007). URB597 and JP104 were purchased from Cayman Chemicals (Ann Arbor, MI). Inhibitors were stored as dry powders at room temperature and dissolved in DMSO to prepare concentrated stock solutions for the *in vitro* potency measurements. SR141716 and SR144528, selective CB1 and CB2 receptor antagonists, were synthesized at Pfizer. Polystyrene 96- and 384-microplates were purchased from Rainin and Evergreen Scientific (Los Angeles, CA), respectively. All reagents used were the highest quality commercially available.

Synthesis of PF-3845 and Structural Analogs

The synthesis of PF-3845 and other biaryl ether piperidine/piperazine ureas was performed as described in Supplemental Experimental Procedures.

FAAH Expression and Purification

All three forms of FAAH (hFAAH, rFAAH, and h/rFAAH) were expressed and purified by following previously described procedures (Mileni et al., 2008) and as described in Supplemental Experimental Procedures.

Determination of Inhibitor Potency

Inhibitor potencies were determined by following previously described procedures (Mileni et al., 2008) and as described in Supplemental Experimental Procedures.

h/rFAAH Crystallography

Crystallization and structure determination were performed as described in Supplemental Experimental Procedures.

Monte Carlo Simulations of FAAH Inhibitor Adducts

The program ICM-Pro (Molsoft, L.L.C.) was used to simulate covalent docking of biaryl ether urea inhibitors into the active site of the h/rFAAH as described in Supplemental Experimental Procedures. As a positive control, we performed the docking of the PF-3845 ligand, which provided a conformation that closely matched the conformation observed in the PF-3845-FAAH crystal structure.

Competitive ABPP Studies

PF-3845 or URB597 (neat) were dissolved at 1 mg/ml by sonication and vortexing directly into a solution of 18:1:1 v/v/v saline:emulphor:ethanol. Male C57Bl/6J mice (6–12 weeks old, 20–28 g) were intraperitoneally (i.p.) administered PF-3845, URB597, or an 18:1:1 v/v/v saline:emulphor:ethanol vehicle at a volume of 10 μ l/g weight (10 mg/kg final dose). After the indicated amount of time, mice were anesthetized with isoflurane and sacrificed by decapitation. Brains were removed and hemisected along the midsagittal plane, and each half was then flash frozen in liquid N₂. One half of the brain was homogenized in PBS (pH 7.4, 2 ml), diluted to 1 mg protein/ml; treated with FP-rhodamine (1 μ M, 0.5 hr); and analyzed by gel-based ABPP by following previously described methods (Alexander and Cravatt, 2005). The other half of the brain was used for lipid and drug measurements as detailed in Supplemental Experimental Procedures.

CC-ABPP Studies

CC-ABPP studies were performed by following previously described procedures (Speers et al., 2003; Speers and Cravatt, 2004; Alexander and Cravatt, 2005) and as detailed in Supplemental Experimental Procedures.

Measurement of FAAH Activity and Lipid Levels from Rat Tissues and Blood Leukocytes

Preparation of rat tissue (brain and liver) and blood leukocytes for measuring FAAH activity and lipid levels is described in Supplemental Experimental Procedures.

Analysis of PF-3845 Effects in the CFA Model of Inflammatory Pain

Male Sprague-Dawley rats (200–250 g) were used for all experiments. Rats were given free access to food and water and were maintained on a 12/12 hr light/dark cycle. For the inflammatory pain model, 0.15 ml CFA (Sigma) was injected into the plantar surface of the left hind paw of the rat. The CFA injection immediately induces local inflammation, paw swelling, and pain, which persist for at least 2 weeks postinjection. To assess mechanical allodynia, mechanical paw-withdrawal thresholds (PWTs) were measured by using a set of Von Frey Hairs on day 5 postinjection as illustrated by the Dixon Up and Down Method (Dixon, 1980). Animals that exhibit the pain criteria of 9 g or less were then placed on study. Test compound was administered via either oral or i.p. routes at the indicated concentrations (mg/kg) with the dosing vehicle 5% *N,N*-dimethylacetamide and 95% 2-hydroxypropyl- β -cyclodextrin (40%) (Sigma) in water. PWTs were evaluated again at 4 hr postdosing. PWT measurements were averaged, and statistical comparisons between groups were made by using analysis of variance and unpaired *t* tests. The Pfizer Institutional Animal Care and Use Committee reviewed and approved the animal use in these studies. The animal care and use program is fully accredited by the Association for Assessment and Accreditation of Laboratory Animal Care, International.

SUPPLEMENTAL DATA

Supplemental Data include Supplemental Experimental Procedures, one table, and five figures and can be found with this article online at [http://www.cell.com/chemistry-biology/supplemental/S1074-5521\(09\)00080-5](http://www.cell.com/chemistry-biology/supplemental/S1074-5521(09)00080-5).

ACKNOWLEDGMENTS

We thank Kimberly Masuda and Jessica P. Alexander for technical assistance with ABPP studies; Max Totrov from Molsoft for helpful suggestions and discussions on the docking and simulation work; Steve Kesten for the scale-up of PF-3845; Mike Walters, Michael Connolly, Yuntao Song, Mark Morris, and Sue Kesten for early chemistry contributions to the biaryl ether series; and Zhigang Wang and Daniel Everdeen for their assistance with the

measurement of inhibitor potencies. This work was supported in part by the National Institutes of Health (DA017259), the Helen L. Dorris Institute for the Study of Neurological and Psychiatric Disorders in Children and Adolescents, and The Skaggs Institute for Chemical Biology.

Received: December 22, 2008

Revised: February 11, 2009

Accepted: February 23, 2009

Published: April 23, 2009

REFERENCES

- Ahn, K., Johnson, D.S., Fitzgerald, L.R., Liimatta, M., Arendse, A., Stevenson, T., Lund, E.T., Nugent, R.A., Nomanbhoy, T.K., Alexander, J.P., and Cravatt, B.F. (2007). Novel mechanistic class of fatty acid amide hydrolase inhibitors with remarkable selectivity. *Biochemistry* **46**, 13019–13030.
- Ahn, K., McKinney, M.K., and Cravatt, B.F. (2008). Enzymatic pathways that regulate endocannabinoid signaling in the nervous system. *Chem. Rev.* **108**, 1687–1707.
- Alexander, J.P., and Cravatt, B.F. (2005). Mechanism of carbamate inactivation of FAAH: implications for the design of covalent inhibitors and in vivo functional probes for enzymes. *Chem. Biol.* **12**, 1179–1187.
- Blankman, J.L., Simon, G.M., and Cravatt, B.F. (2007). A comprehensive profile of brain enzymes that hydrolyze the endocannabinoid 2-arachidonoyl-glycerol. *Chem. Biol.* **14**, 1347–1356.
- Boger, D.L., Sato, H., Lerner, A.E., Austin, B.J., Patterson, J.E., Patricelli, M.P., and Cravatt, B.F. (1999). Trifluoromethyl ketone inhibitors of fatty acid amide hydrolase: a probe of structural and conformational features contributing to inhibition. *Bioorg. Med. Chem. Lett.* **9**, 265–270.
- Boger, D.L., Sato, H., Lerner, A.E., Hedrick, M.P., Cecik, R.A., Miyauchi, H., Wilkie, G.D., Austin, B.J., Patricelli, M.P., and Cravatt, B.F. (2000). Exceptionally potent inhibitors of fatty acid amide hydrolase: the enzyme responsible for degradation of endogenous oleamide and anandamide. *Proc. Natl. Acad. Sci. USA* **97**, 5044–5049.
- Bracey, M.H., Hanson, M.A., Masuda, K.R., Stevens, R.C., and Cravatt, B.F. (2002). Structural adaptations in a membrane enzyme that terminates endocannabinoid signaling. *Science* **298**, 1793–1796.
- Brandl, M., Weiss, M.S., Jabs, A., Suhnel, J., and Hilgenfeld, R. (2001). C-H...pi-interactions in proteins. *J. Mol. Biol.* **307**, 357–377.
- Chang, L., Luo, L., Palmer, J.A., Sutton, S., Wilson, S.J., Barbier, A.J., Breitenbucher, J.G., Chaplan, S.R., and Webb, M. (2006). Inhibition of fatty acid amide hydrolase produces analgesia by multiple mechanisms. *Br. J. Pharmacol.* **148**, 102–113.
- Cravatt, B.F., Giang, D.K., Mayfield, S.P., Boger, D.L., Lerner, R.A., and Gilula, N.B. (1996). Molecular characterization of an enzyme that degrades neuromodulatory fatty-acid amides. *Nature* **384**, 83–87.
- Cravatt, B.F., Demarest, K., Patricelli, M.P., Bracey, M.H., Giang, D.K., Martin, B.R., and Lichtman, A.H. (2001). Supersensitivity to anandamide and enhanced endogenous cannabinoid signaling in mice lacking fatty acid amide hydrolase. *Proc. Natl. Acad. Sci. USA* **98**, 9371–9376.
- Cravatt, B.F., Saghatelian, A., Hawkins, E.G., Clement, A.B., Bracey, M.H., and Lichtman, A.H. (2004). Functional disassociation of the central and peripheral fatty acid amide signaling systems. *Proc. Natl. Acad. Sci. USA* **101**, 10821–10826.
- Deutsch, D.G., Omir, R., Arreaza, G., Salehani, D., Prestwich, G.D., Huang, Z., and Howlett, A. (1997). Methyl arachidonoyl fluorophosphonate: a potent irreversible inhibitor of anandamide amidase. *Biochem. Pharmacol.* **53**, 255–260.
- Di Marzo, V. (2008). Endocannabinoids: synthesis and degradation. *Rev. Physiol. Biochem. Pharmacol.* **160**, 1–24.
- Di Marzo, V., Bisogno, T., and De Petrocellis, L. (2007). Endocannabinoids and related compounds: walking back and forth between plant natural products and animal physiology. *Chem. Biol.* **14**, 741–756.
- Dixon, W.J. (1980). Efficient analysis of experimental observations. *Annu. Rev. Pharmacol. Toxicol.* **20**, 441–462.
- Fegley, D., Gaetani, S., Duranti, A., Tontini, A., Mor, M., Tarzia, G., and Piomelli, D. (2005). Characterization of the fatty acid amide hydrolase inhibitor cyclohexyl carbamic acid 3'-carbamoyl-biphenyl-3-yl ester (URB597): effects on anandamide and oleylethanolamide deactivation. *J. Pharmacol. Exp. Ther.* **313**, 352–358.
- Fowler, C.J. (2006). The cannabinoid system and its pharmacological manipulation—a review, with emphasis upon the uptake and hydrolysis of anandamide. *Fundam. Clin. Pharmacol.* **20**, 549–562.
- Glaser, S.T., Kaczocha, M., and Deutsch, D.G. (2005). Anandamide transport: a critical review. *Life Sci.* **77**, 1584–1604.
- Gobbi, G., Bambico, F.R., Mangieri, R., Bortolato, M., Campolongo, P., Solinas, M., Cassano, T., Morgese, M.G., Debonnel, G., Duranti, A., et al. (2005). Antidepressant-like activity and modulation of brain monoaminergic transmission by blockade of anandamide hydrolysis. *Proc. Natl. Acad. Sci. USA* **102**, 18620–18625.
- Hillard, C.J., and Jarrahan, A. (2003). Cellular accumulation of anandamide: consensus and controversy. *Br. J. Pharmacol.* **140**, 802–808.
- Holt, S., Comelli, F., Costa, B., and Fowler, C.J. (2005). Inhibitors of fatty acid amide hydrolase reduce carrageenan-induced hind paw inflammation in pentobarbital-treated mice: comparison with indomethacin and possible involvement of cannabinoid receptors. *Br. J. Pharmacol.* **146**, 467–476.
- Jayamanne, A., Greenwood, R., Mitchell, V.A., Aslan, S., Piomelli, D., and Vaughan, C.W. (2006). Actions of the FAAH inhibitor URB597 in neuropathic and inflammatory chronic pain models. *Br. J. Pharmacol.* **147**, 281–288.
- Kathuria, S., Gaetani, S., Fegley, D., Valino, F., Duranti, A., Tontini, A., Mor, M., Tarzia, G., La Rana, G., Calignano, A., et al. (2003). Modulation of anxiety through blockade of anandamide hydrolysis. *Nat. Med.* **9**, 76–81.
- Keith, J.M., Apodaca, R., Xiao, W., Seierstad, M., Pattabiraman, K., Wu, J., Webb, M., Karbarz, M.J., Brown, S., Wilson, S., et al. (2008). Thiadiazolopiperazinyl ureas as inhibitors of fatty acid amide hydrolase. *Bioorg. Med. Chem. Lett.* **18**, 4838–4843.
- Koutek, B., Prestwich, G.D., Howlett, A.C., Chin, S.A., Salehani, D., Akhavan, N., and Deutsch, D.G. (1994). Inhibitors of arachidonoyl ethanolamide hydrolysis. *J. Biol. Chem.* **269**, 22937–22940.
- Lambert, D.M., Vandevoorde, S., Jonsson, K.O., and Fowler, C.J. (2002). The palmitoylethanolamide family: a new class of anti-inflammatory agents? *Curr. Med. Chem.* **9**, 663–674.
- Leung, D., Hardouin, C., Boger, D.L., and Cravatt, B.F. (2003). Discovering potent and selective inhibitors of enzymes in complex proteomes. *Nat. Biotechnol.* **21**, 687–691.
- Leung, D., Saghatelian, A., Simon, G.M., and Cravatt, B.F. (2006). Inactivation of N-acyl ethanolamine phospholipase D reveals multiple mechanisms for the biosynthesis of endocannabinoids. *Biochemistry* **45**, 4720–4726.
- Lichtman, A.H., Leung, D., Shelton, C., Saghatelian, A., Hardouin, C., Boger, D., and Cravatt, B.F. (2004a). Reversible inhibitors of fatty acid amide hydrolase that promote analgesia: evidence for an unprecedented combination of potency and selectivity. *J. Pharmacol. Exp. Ther.* **311**, 441–448.
- Lichtman, A.H., Shelton, C.C., Advani, T., and Cravatt, B.F. (2004b). Mice lacking fatty acid amide hydrolase exhibit a cannabinoid receptor-mediated phenotypic hypoalgesia. *Pain* **109**, 319–327.
- Liu, Y., Patricelli, M.P., and Cravatt, B.F. (1999). Activity-based protein profiling: the serine hydrolases. *Proc. Natl. Acad. Sci. USA* **96**, 14694–14699.
- Long, J.Z., Li, W., Booker, L., Burston, J.J., Kinsey, S.G., Schlosburg, J.E., Pavan, F.J., Serrano, A.M., Selley, D.E., Parsons, L.H., et al. (2009). Selective blockade of 2-arachidonoylglycerol hydrolysis produces cannabinoid behavioral effects. *Nat. Chem. Biol.* **5**, 37–44.
- Massa, F., Marsicano, G., Hermann, H., Cannich, A., Monory, K., Cravatt, B.F., Ferri, G.L., Sibaev, A., Storr, M., and Lutz, B. (2004). The endogenous cannabinoid system protects against colonic inflammation. *J. Clin. Invest.* **113**, 1202–1209.
- McFarland, M.J., and Barker, E.L. (2004). Anandamide transport. *Pharmacol. Ther.* **104**, 117–135.
- McKinney, M.K., and Cravatt, B.F. (2005). Structure and function of fatty acid amide hydrolase. *Annu. Rev. Biochem.* **74**, 411–432.

- Mechoulam, R. (1986). *The Pharmacohistory of Cannabis sativa* (Boca Raton, FL: CRS Press).
- Mileni, M., Johnson, D.S., Wang, Z., Everdeen, D.S., Liimatta, M., Pabst, B., Bhattacharya, K., Nugent, R.A., Kamtekar, S., Cravatt, B.F., et al. (2008). Structure-guided inhibitor design for human FAAH by interspecies active site conversion. *Proc. Natl. Acad. Sci. USA* *105*, 12820–12824.
- Moreira, F.A., Kaiser, N., Monory, K., and Lutz, B. (2008). Reduced anxiety-like behaviour induced by genetic and pharmacological inhibition of the endocannabinoid-degrading enzyme fatty acid amide hydrolase (FAAH) is mediated by CB1 receptors. *Neuropharmacology* *54*, 141–150.
- Naidu, P.S., Varvel, S.A., Ahn, K., Cravatt, B.F., Martin, B.R., and Lichtman, A.H. (2007). Evaluation of fatty acid amide hydrolase inhibition in murine models of emotionality. *Psychopharmacology (Berl.)* *192*, 61–70.
- Nomura, D.K., Blankman, J.L., Simon, G.M., Fujioka, K., Issa, R.S., Ward, A.M., Cravatt, B.F., and Casida, J.E. (2008). Activation of the endocannabinoid system by organophosphorus nerve agents. *Nat. Chem. Biol.* *4*, 373–378.
- Pacher, P., Batkai, S., and Kunos, G. (2006). The endocannabinoid system as an emerging target of pharmacotherapy. *Pharmacol. Rev.* *58*, 389–462.
- Patricelli, M.P., Lovato, M.A., and Cravatt, B.F. (1999). Chemical and mutagenic investigations of fatty acid amide hydrolase: evidence for a family of serine hydrolase with distinct catalytic features. *Biochemistry* *38*, 9804–9812.
- Patricelli, M.P., Giang, D.K., Stamp, L.M., and Burbaum, J.J. (2001). Direct visualization of serine hydrolase activities in complex proteome using fluorescent active site-directed probes. *Proteomics* *1*, 1067–1071.
- Russo, R., Loverme, J., La Rana, G., Compton, T.R., Parrott, J., Duranti, A., Tontini, A., Mor, M., Tarzia, G., Calignano, A., and Piomelli, D. (2007). The fatty acid amide hydrolase inhibitor URB597 (cyclohexylcarbamic acid 3'-carbamoylbiphenyl-3-yl ester) reduces neuropathic pain after oral administration in mice. *J. Pharmacol. Exp. Ther.* *322*, 236–242.
- Saghatelian, A., Trauger, S.A., Want, E.J., Hawkins, E.G., Siuzdak, G., and Cravatt, B.F. (2004). Assignment of endogenous substrates to enzymes by global metabolite profiling. *Biochemistry* *43*, 14332–14339.
- Speers, A.E., and Cravatt, B.F. (2004). Profiling enzyme activities in vivo using click chemistry methods. *Chem. Biol.* *11*, 535–546.
- Speers, A.E., Adam, G.C., and Cravatt, B.F. (2003). Activity-based protein profiling in vivo using a copper(I)-catalyzed azide-alkyne [3 + 2] cycloaddition. *J. Am. Chem. Soc.* *125*, 4686–4687.
- Swinney, D.C. (2004). Biochemical mechanisms of drug action: what does it take for success? *Nat. Rev. Drug Discov.* *3*, 801–808.
- Tsuboi, K., Sun, Y.X., Okamoto, Y., Araki, N., Tonai, T., and Ueda, N. (2005). Molecular characterization of N-acyl ethanolamine-hydrolyzing acid amidase, a novel member of the cholineglycine hydrolase family with structural and functional similarity to acid ceramidase. *J. Biol. Chem.* *280*, 11082–11092.
- Wei, B.Q., Mikkelsen, T.S., McKinney, M.K., Lander, E.S., and Cravatt, B.F. (2006). A second fatty acid amide hydrolase with variable distribution among placental mammals. *J. Biol. Chem.* *281*, 36569–36578.
- Zhang, D., Saraf, A., Kolasa, T., Bhatia, P., Zheng, G.Z., Patel, M., Lannoye, G.S., Richardson, P., Stewart, A., Rogers, J.C., et al. (2007). Fatty acid amide hydrolase inhibitors display broad selectivity and inhibit multiple carboxylesterases as off-targets. *Neuropharmacology* *52*, 1095–1105.